Kinetic Analysis of Interdomain Coupling in a Lidless Variant of the Molecular Chaperone DnaK: DnaK's Lid Inhibits Transition to the Low Affinity State†

Sergey V. Slepenkov and Stephan N. Witt*

Department of Biochemistry and Molecular Biology, Louisiana State University Medical Center, 1501 Kings Highway, Shreveport, Louisiana 71130-3932

Received June 18, 2002; Revised Manuscript Received August 4, 2002

ABSTRACT: DnaK, the *Escherichia coli* Hsp70, possesses two functional domains, the N- and C-terminal ATPase and peptide-binding domains, respectively. Elucidation of the mechanism of allosteric coupling between the two domains is key to understanding how Hsp70 chaperones interact with their substrates. We previously reported that ATP reacts with wild-type DnaK−peptide complexes according to the two-step reaction, ATP + DnaK−P ⇔ ATP−DnaK−P ⇔ ATP−DnaK* + P, where ATP binds in the first step, and a conformational change that quenches DnaK's tryptophan fluorescence (denoted by the asterisk) and expels bound peptide occurs in the second step. Here we report that DnaK(2-517), a lidless variant, also reacts with ATP and peptide by this two-step mechanism. Compared to wild-type DnaK, we found that, depending on the sequence of the bound peptide and the temperature, deletion of the lid produces a 27- to 66-fold increase in the rate constant (k_2) for the ATP-triggered conformational change (ATP−DnaK−P → ATP−DnaK*+P) but only a ∼2-fold increase in the rate constant (k_{-2}) for the reverse reaction (ATP−DnaK*+P → ATP−DnaK−P). A model is proposed in which the lid regulates the rate of interdomain communication by retarding motions within the β-sandwich that occur as a consequence of ATP binding. New evidence in support of the reversible, two-step conformational switch mechanism is also presented.

The *Escherichia coli* Hsp70 chaperone DnaK promotes a variety of essential reactions in the cell, such as the folding, assembly, transport, and proteolysis of other proteins (for reviews, see refs *1*−*5*). In these different reactions, it is thought that DnaK and other members of the Hsp70 family selectively bind partially unfolded or disordered regions of other proteins in an activity cycle that is controlled by the binding and hydrolysis of ATP. The mechanism by which the binding and hydrolysis of ATP is coupled to the binding, retention, and release of polypeptides by these molecular chaperones is not known.

DnaK is composed of two functional domains: residues 1−387 comprise the N-terminal domain, which binds and hydrolyzes ATP (*6*), whereas residues 388−638 comprise the C-terminal domain (Figure 1), which binds and releases polypeptide targets (*7*, *8*). A subdomain composed of five α helices (residues 507−638) serves as a lid-like device that encapsulates the bound peptide in the ADP-bound state. The hallmark of the Hsp70 reaction cycle is that the activities of these two functional domains are coupled; i.e., ligand-induced conformational changes are transmitted in a reciprocal fashion between the two domains. As examples, ATP binding triggers the rapid release of peptide substrates from the peptide-binding domain (*9*, *10*). Conversely, peptide binding triggers a rapid global conformational change in DnaK (*11*), which results in accelerated DnaK-mediated ATP hydrolysis (*12*−*14*). From recent work it is now known that interdomain coupling occurs even when the lid is deleted (*15*−*17*).

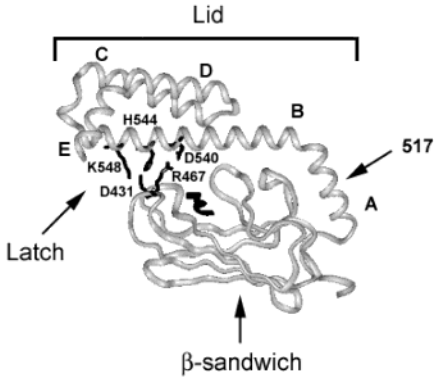

FIGURE 1: Structure of the polypeptide-binding domain (residues 394−607) of DnaK. The bound NR peptide (NRLLLTG) is depicted in black. The arrow indicates residue 517. The lid is latched to the β-sandwich via a network of hydrogen bonds. The amino acids that participate in the network are indicated. The five α-helices that comprise the lid are labeled A−E. The image was constructed from PDB file 1DKX.

An excellent way to study the allosteric coupling between the two domains is to follow the kinetics of the ATP-induced conformational change in DnaK by monitoring changes in tryptophan fluorescence (*18*, *19*). The presence of only one tryptophan residue (*20*), Trp^{102}, which is in close proximity to the ATP binding site, simplifies the interpretation of the spectral changes. It has been shown that in the absence of added peptide the binding of ATP to nucleotide-free DnaK results in two phases of tryptophan fluorescence quenching (*19*). The first and second phases are characterized by maximal apparent first-order rate constants of 19 and 0.67 s^{-1}, respectively. The reaction kinetics in this special case

† Support for this work came from the NIH (GM 51521).

* To whom correspondence should be addressed. Tel: (318) 675-7891 FAX: (318) 675-5180. E-Mail: switt1@ lsuhsc.edu

10.1021/bi0263208 CCC: $22.00
Published on Web 09/13/2002

are consistent with a three-step mechanism. On the other hand, when ATP is mixed with DnaK−peptide complexes, tryptophan fluorescence quenching occurs in a single phase (*11*, *18*) with $k_{obs} \approx 3-6\ s^{-1}$. A detailed kinetic analysis of the reaction between ATP with nucleotide-free DnaK−peptide complexes revealed a hyperbolic dependence of k_{obs} on [ATP] (*11*). The results are consistent with the minimal two-step mechanism

$$\text{ATP} + \text{DnaK}\cdot\text{P} \underset{k_{-1}^{ATP}}{\overset{k_1^{ATP}}{\rightleftharpoons}} \text{ATP}\cdot\text{DnaK}\cdot\text{P} \underset{k_{-2}}{\overset{k_2}{\rightleftharpoons}} \text{ATP}\cdot\text{DnaK}^* + \text{P} \quad (1)$$

DnaK·P and ATP·DnaK* are the high- and low-affinity states of DnaK, respectively, and ATP·DnaK·P is an intermediate. A rapid equilibrium between DnaK and ATP occurs in the first step, whereas a global conformational change that reduces the fluorescence and simultaneously expels bound peptide occurs in the second step. Interestingly, the reverse reaction, mixing ATP-bound DnaK (ATP·DnaK*) with unlabeled peptide, results in a rapid increase in tryptophan fluorescence (*11*). Because the rate of the peptide-induced increase in tryptophan fluorescence is far faster than the rate of DnaK-mediated ATP hydrolysis, the second step of reaction 1, the conformational switch, occurs in the forward and reverse directions without the hydrolysis of ATP.

It is possible that the second step of reaction 1 consists of two steps:

$$\text{ATP} + \text{DnaK}\cdot\text{P} \underset{k_{-1}^{ATP}}{\overset{k_1^{ATP}}{\rightleftharpoons}} \text{ATP}\cdot\text{DnaK}\cdot\text{P} \underset{k_{-2}}{\overset{k_2}{\rightleftharpoons}} \text{ATP}\cdot\text{DnaK}^*\cdot\text{P} \underset{k_{-3}}{\overset{k_3}{\rightleftharpoons}} \text{ATP}\cdot\text{DnaK}^* + \text{P} \quad (2)$$

A rapid equilibrium between DnaK·P and ATP, a global conformational change in DnaK (that reduces tryptophan fluorescence, as denoted by the asterisk), and rapid peptide dissociation/association define these three steps. If $k_3 \gg k_2$, then the ATP-triggered conformational change in the protein limits the rate of peptide release. Because there is no evidence, to date, for an ATP·DnaK*·P intermediate, the data in this study are interpreted according to the above two-step mechanism 1. That said, the rate constants determined here are microscopic rate constants if, and only if, reaction 2 can be eliminated as a possible mechanism. In this regard, simulations of reactions 1 and 2, in the Appendix, indicate differences between these two mechanisms which support the two-step model for the interaction of DnaK with ATP and peptide.

We show here that deletion of residues 518−638, which constitute nearly all five helices of DnaK's lid, dramatically increases k_2 but leaves k_{-2} relatively unaffected. Without the lid, DnaK's ability to bind substrates polypeptides is severely compromised, especially at elevated temperatures.

MATERIALS AND METHODS

Protein and Reagents. All reagents were of the highest purity and were purchased from Sigma, unless stated otherwise. DnaK was isolated as previously described (*16*) and stored at 4 °C in the sample buffer (25 mM *N*-(2-hydroxyethyl)piperazine-*N*′-2-ethanesulfonic acid/50 mM KCl/5 mM $MgCl_2$/5 mM 2-mercaptoethanol at pH 7.0). Nucleotide was removed from wtDnaK and DnaK(2−517) either by exhaustive dialysis (*21*) or the method of Gao et al. that employs AMP−PNP (*22*). Protein was stored in the HEPES sample buffering containing 10% glycerol at −80 °C prior to use.

Construction of the DnaK(1−517) Expressing Plasmid. We previously reported the preparation of an N-terminal, glutathione S-transferase (GST) tagged version of DnaK-(1−517) (*17*). In this study PCR mutagenesis was used to create a different plasmid, one that eliminated the need for the GST fusion. The pMSK plasmid harboring the wild type *dnaK* gene behind an IPTG inducible promoter was a gift to us from Lila Gierasch (University of Massachusetts, Amherst). Using the QuikChange Site-Directed Mutagenesis Kit (Stratagene), a stop codon was introduced into the *dnaK* gene such that translation terminates at residue 517. The forward and reverse primers were 5′-CAGAAAATGGTACGC-TAAGCAGAAGCTAACGCC-3′ and 5′-GGCGTTAGCT-TCTGCTTAGCGTACCATTTTCTG-3′, respectively. To ensure that a secondary mutation was not introduced during the PCR protocol, the gene encoding DnaK(1−517) in the pDnaK517 plasmid was sequenced at the Iowa State University DNA Sequencing & Synthesis Facility. This lidless variant of DnaK was expressed in the DnaK deficient *E. coli* strain BB1553 (*23*) and purified using the same methods as the wild-type protein. N-terminal sequencing (Macromolecular Structure Analysis Facility, University of Kentucky, Lexington) revealed that Met[1] is absent from both the lidless and wild-type proteins. We refer below to the lidless variant of DnaK that lacks residues 1 and 518−638 as DnaK(2−517).

Peptides were purchased from Genemed Synthesis Incorporated (S. San Francisco, CA), purified to >95% by high performance liquid chromatography, and peptide mass was verified by electrospray mass spectroscopy. The NR (NR-LLLTG) and p5 (CLLLSAPRR) peptides were the primary peptides used in this study. The NR peptide (*24*) was dansylated at its N-terminus as described (*17*), and the p5 peptide (*25*) was labeled at the cysteine residue with acrylodan and subsequently purified as described (*10*, *26*). The dansyl-NR and acrylodan-p5 peptides are referred to as fNR and ap5, respectively. Masses of the labeled peptides were verified by electrospray mass spectrometry. Control experiments showed that unlabeled peptide competitively inhibits the binding of each labeled peptide to DnaK.

Kinetic Methods. A SX-18MV stopped-flow fluorescence spectrometer (Applied Photophysics Ltd (Leatherhead, U.K.) was used to monitor spectral changes that occur in both the forward and reverse reactions. The dead-time of the instrument was 1.5 ms, and the dimensions of the optical cell where mixing and detection occurs equaled 1 cm × 0.2 cm × 0.1 cm. Excitation occurred through the 0.2 cm path and detection through the 0.1 cm path. The conditions under which the several different types of rapid kinetic experiments

[1] Abbreviations: NR, synthetic peptide NRLLLTG; fNR, α-*N*, dansyl-NR peptide; acrylodan, a, 6-acryloyl-2-(dimethylamino)naphthalene; p5, synthetic peptide CLLLSAPRR; ap5, acrylodan-labeled p5 peptide; HEPES, *N*-(2-hydroxyethyl) piperazine-*N*′-2-ethanesulfonic acid.

were the same as those previously described (*11*). For most stopped-flow experiments, the instrumental time constant was equal to 5% of the reaction half-time. For the case of very fast reactions, no in-line filtering was used. Each stopped-flow trace is the average of 4−10 individual traces. In some cases, data were collected using a split time base mode. Temperature control of both the jacketed reactants and the jacketed mixing chamber was achieved with a circulating external water bath ($\Delta T = \pm 0.2$ °C). The concentrations in the text refer to after mixing.

Forward Reaction: ATP-Induced Peptide Dissociation from DnaK. Fluorescent peptide dissociation from preformed DnaK·fluorescent peptide (ap5 or fNR) complexes was probed using a stopped-flow spectrometer with fluorescence detection. ATP (0.01−16 mM) and unlabeled peptide (10 μM) were contained in one syringe, and DnaK (2 μM) and ap5 or fNR (0.1 μM) were contained in the other syringe. For the case of DnaK(2−517), where much higher concentrations of ATP were used, [$MgCl_2$] = 20 mM after mixing. The solution of protein and peptide was allowed to preincubate for 2 h at the desired temperature in order to form the protein-fluorescent peptide complexes.

When excess unlabeled peptide is contained in the syringe with ATP, rebinding of the fluorescent peptide is negligible ($k_{-2} \times$ [fP*] ≈ 0), thus peptide dissociation occurs according to

$$\mathrm{ATP} + \mathrm{DnaK{\cdot}fP} \underset{k_{-1}^{\mathrm{ATP}}}{\overset{k_1^{\mathrm{ATP}}}{\rightleftharpoons}} \mathrm{ATP{\cdot}DnaK{\cdot}fP} \xrightarrow{k_2} \mathrm{ATP{\cdot}DnaK} + \mathrm{fP}^* \quad (3)$$

The fluorescently tagged peptide is less fluorescent when free in solution as compared to that when DnaK-bound. This reduced fluorescence is denoted by the asterisk. Upon mixing, the decrease in fluorescence due to the dissociation of the bound fluorescent peptide followed the equation

$$F(t) = \Delta F e^{-k_{\mathrm{obs}}^{\mathrm{off}} t} + F_\infty \quad (4)$$

where $k_{\mathrm{obs}}^{\mathrm{off}}$, ΔF, and F_∞ are the observed first-order off-rate constant, amplitude, and final fluorescence, respectively. Kinetic parameters were extracted from the observed dissociation rate constants using the following equation, which was derived by applying the steady-state approximation. In the equation below, $K_{\mathrm{app}} = (k_{-1}^{\mathrm{ATP}} + k_2)/k_1^{\mathrm{ATP}}$:

$$k_{\mathrm{obs}}^{\mathrm{off}} = \frac{k_2[\mathrm{ATP}]}{K_{\mathrm{app}} + [\mathrm{ATP}]} \quad (5)$$

For the ap5 peptide, the excitation wavelength was 370 nm (2.5 nm bandwidth), and stray excitation radiation was eliminated with a 470 nm Oriel long-pass filter. For the fNR peptide, the excitation wavelength was 335 nm (2.5 nm bandwidth), and stray excitation radiation was eliminated with a 399 nm Oriel long-pass filter.

Reverse Reaction: Peptide Binding to ATP-Bound DnaK. The binding of the p5 or NR peptide to the low affinity state of DnaK was probed using a stopped-flow spectrometer to follow the increase in DnaK's tryptophan fluorescence that occurs on peptide binding

$$\mathrm{ATP{\cdot}DnaK}^* + \mathrm{P} \underset{k_2}{\overset{k_{-2}}{\rightleftharpoons}} \mathrm{ATP{\cdot}DnaK{\cdot}P} \quad (6)$$

The low-affinity state of DnaK was prepared by mixing wtDnaK (2 μM) with excess ATP (1 mM) in buffers containing 5 mM $MgCl_2$ or by mixing DnaK(2−517) (2 μM) with 8 mM ATP in the presence of 20 mM $MgCl_2$. One syringe was loaded with the solution of low affinity complexes and the other with varying amounts of the unlabeled peptide (5−200 μM) with 1 or 8 mM ATP. The peptide-induced increase in the tryptophan fluorescence of wtDnaK or DnaK(2−517) followed

$$F(t) = \Delta F(1 - e^{-k_{\mathrm{obs}}^{\mathrm{on}} t}) + F_o \quad (7)$$

where $k_{\mathrm{obs}}^{\mathrm{on}}$, ΔF, and F_o are the observed first-order rate constant, amplitude, and initial fluorescence, respectively. For binding according to reaction 6, with [P] ≫ [ATP·DnaK*], $k_{\mathrm{obs}}^{\mathrm{on}} = k_{-2}[\mathrm{P}] + k_2$.

The excitation wavelength was 295 nm (1.5 or 2.5 nm bandwidth), and stray excitation radiation was eliminated with either a 320 or 335 nm Oriel long-pass filter. The following control experiments were conducted: (i) No increase in tryptophan fluorescence was observed when either wtDnaK or DnaK(2−517) was rapidly mixed with excess p5 or NR peptide; (ii) as a negative control, when ATP-bound DnaK (ATP·wtDnaK*) was rapidly mixed with 200 μM poly-glutamic acid, no increase in tryptophan fluorescence was observed. (It was expected that poly-glutamic acid would not bind ATP-bound DnaK because DnaK is known to weakly interact with peptides that contain negatively charged residues (*24*). If there is no binding, there should be no increase in tryptophan fluorescence upon mixing.)

Experiments were also conducted in which complex formation between ap5 and ATP-bound DnaK was monitored by following the increase in acrylodan fluorescence that occurs upon complex formation. In these experiments, the concentration of ATP-bound DnaK was varied at a fixed concentration of ap5 ([ATP−DnaK]≫[ap5]). Experiments were the same as described above except that the excitation wavelength was 370 nm (1.5 or 2.5 nm bandwidth), and stray excitation radiation was eliminated with a 470 nm Oriel long-pass filter. Formation traces followed eq 7, and $k_{\mathrm{obs}}^{\mathrm{on}} = k_{-2}[\mathrm{ATP{-}DnaK}] + k_2$.

To estimate how much ADP was generated while DnaK (2 μM) and ATP (1 mM) incubated in the stopped-flow syringe, the measured value for k_{cat}(25 °C) (3.6×10^{-2} μmol ATP (μmol DnaK)$^{-1}$ min^{-1} at pH 7.0) was used to estimate k_{cat} values at 15 °C and 5 °C, using

$$k_{\mathrm{cat}}(T_1) = k_{\mathrm{cat}}(298\ \mathrm{K}) \exp\left[\frac{-\Delta \mathrm{H}^*}{R}\left(\frac{1}{T_1} - \frac{1}{298}\right)\right] \quad (8)$$

In the above equation, ΔH^* equals 25.0 kcal/mol (*19*), $R = 1.987 \times 10^{-3}$ kcal mol^{-1} K^{-1}, and $T_1 = 288$ or 278 K. Calculated values for k_{cat}(15 °C) and k_{cat}(5 °C) are 8.3×10^{-3} min^{-1} and 1.9×10^{-3} min^{-1}, respectively. Using these k_{cat} values, wtDnaK-catalyzed ATP hydrolysis produced very small quantities of ADP during the short residence time in the syringe. Specifically, 0.057, 0.25, and 1.1 μM (= 2 μM DnaK × 15 min × 3.6×10^{-2} μmol ATP (μmol DnaK)$^{-1}$

min^{-1}) of ADP are generated after a 15 min incubation at 5, 15, and 25 °C, respectively. When [ATP] ≫ [ADP], the occupation of DnaK with ATP is calculated according to the following equation (*27*):

$$\frac{[\text{DnaK·ATP}]}{[\text{DnaK}]_{tot}} = \frac{k_{off}^{ADP}}{k_{off}^{ADP} + k_{cat}} \quad (9)$$

Reported values for k_{off}^{ADP} at 15 and 25 °C are 2.2×10^{-2} s^{-1} and 1.2×10^{-2} s^{-1}, respectively (*19*). Using eq 8 to estimate k_{off}^{ADP}(5 °C), with $\Delta H^* = 9.7$ kcal/mol (*19*), yields k_{off}^{ADP}(5 °C) = 6.8×10^{-3} s^{-1}. Using eq 9, we calculate that 99.5, 98.9, and 97.3% of the DnaK molecules are ATP-bound after a 15 min incubation at 5, 15, and 25 °C, respectively. Because DnaK(2−517) exhibits nearly the same k_{cat}(25 °C) as wild type and because ADP dissociates from DnaK(2−517) with nearly the same rate constants as wild type, approximately the same percent of ATP-bound DnaK(2−517) occurs after a 15 min incubation.

ATPase Activity Assay. The steady-state rate of DnaK-mediated ATP hydrolysis (k_{cat}[μmol ATP (μmol of DnaK)$^{-1}$ min^{-1}]) was measured by separating [2,8-^{3}H] ATP from [2,8-^{3}H] ADP using PEI cellulose plates as previously described (*17*). The k_{cat} values used in the Arrhenius plots were obtained at saturating concentrations of added peptide ([NR], [p5] = 1 mM).

Curve Fitting and Error Analysis. Stopped-flow data were fitted to single-exponential function using a curve fitting program that used a Marquardt algorithm based on the program Curfit given in Bevington (*28*). Least-squares fitting of data to hyperbolic or linear equations and determinations of standard errors of the fitted parameters were conducted using the program KaleidaGraph (Synergy Software, Reading, PA). Dissociation traces obtained at low concentrations of ATP and low temperatures exhibited a slight deviation from single-exponential kinetics, as described below. Our simulations of reaction 3, using the program KINSIM (*29*), also show a slight lag phase in the simulated traces at low ATP concentrations and for small values of k_2 (<2 s^{-1}). For each trace with this short lag phase, the fit to eq 4 was started right after the lag phase. According to our simulations of reaction 3, this approximation results in a ∼10% error in the reported values for K_{app}.

RESULTS

The purpose of this study was to elucidate how the lid affects interdomain coupling in the molecular chaperone DnaK. Wild-type DnaK and DnaK(2−517), which lacks residues 518−638, were used in this study. Before conducting the kinetic experiments, our initial characterization of DnaK(2−517) (M. Sehorn and S. Witt, unpublished results) showed that (i) the circular dichroism spectrum of DnaK(2−517), with two intense negative bands at 208 and 222 nm, is similar to that of the wild type protein. Thus, loss of the lid therefore does not create a partially denatured protein. (ii) Unlike wtDnaK, DnaK(2−517) exhibits no appreciable self-association, as judged from high performance size exclusion chromatography. (iii) The hydrophobic dye ANS (1-anilino-naphthalene-8-sulfonate) shows no appreciable binding to either wtDnaK or DnaK(2−517) at pH 7.0, which is evidence for a compact state of the lidless protein in which the hydrophobic core of the protein is inaccessible. Additionally, a related DnaK variant, DnaK(2−507), functions in vivo, albeit with reduced activity compared to wild-type DnaK (*15*). The results show that DnaK(2−517) exists in a compact, active conformation.

Forward Reaction: ATP-Triggered Peptide Dissociation from Preformed DnaK·Peptide Complexes. A basic question is whether DnaK(2−517) interacts with ATP and peptide according to reaction 1. One way to answer this is to measure the rate of peptide dissociation from DnaK or DnaK(2−517) as a function of ATP concentration using a stopped-flow instrument. If DnaK(2−517) reacts according to the two-step mechanism, then a plot of k_{obs}^{off} versus [ATP] should be hyperbolic (eq 5). These dissociation experiments consisted of rapidly mixing preformed nucleotide-free DnaK·ap5 complexes with ATP and excess unlabeled peptide. The acrylodan fluorescence signal decreases as the peptide dissociates.

Panles A and B of Figure 2 show traces for ap5 dissociation from preformed wtDnaK·ap5 and DnaK(2−517)·ap5 complexes, respectively. The dissociation traces for each protein were fitted to a single-exponential function (eq 4), yielding values for the observed first-order off-rate constant (k_{obs}^{off}). Dissociation traces for the wild-type protein exhibit a slight deviation from the single-exponential fit for [ATP] < 40 μM, and no improvement in fit occurs when a double exponential function is used (Figure 2, top of panel A). The deviation from the single-exponential fit is due to the presence of a slight lag phase at low ATP concentrations and low temperatures. Such a lag phase, which is expected for sequential reaction 3, is due to the time required to reach the maximum concentration of the intermediate complex ATP·DnaK·P (*30*). The large values for k_2 observed for DnaK(2−517) significantly shorten the time required to reach the maximal concentration of the intermediate on mixing; thus, no lag phase is apparent over the time scale of the measurements (Figure 2B). For [ATP] < 40 μM, at 5 and 15 °C, values for k_{obs}^{off} were estimated by using a single exponential to fit each trace commencing just after the lag phase (Figure 2, residual top of panel A). For [ATP] ≥ 40 μM, at each temperature, all dissociation traces, commencing at the zero point, fit a single-exponential function. In general, ap5 dissociation from DnaK(2−517) was about ∼10-fold faster at a given ATP concentration as compared to the wild-type protein. For example, at 40 μM ATP k_{obs}^{off} equals 0.40 and 5.2 s^{-1}, respectively, for ap5 dissociation from wtDnaK and DnaK(2−517).

The k_{obs}^{off} values determined from the above experiments are plotted against ATP concentration in Figure 2C,D. The hyperbolic nature of the plots is consistent with two-step ATP binding to DnaK (eq 1), with peptide kick-off occurring in the second step (*11*, *18*). Fits of the data to eq 5 yield the parameters K_{app} and k_2. At 5 °C, for the wild-type protein, the parameters K_{app} and k_2 equal 3.2 μM and 0.44 s^{-1} respectively, whereas for DnaK(2−517), K_{app} and k_2 equal 100 μM and 18.4 s^{-1} respectively. Table 1 gives K_{app} and k_2 values, which were determined over a range of temperatures, for ap5 dissociation from wtDnaK and DnaK(2−517). For comparison, Table 2 gives the same parameters but for the NR peptide (NRLLLTG).

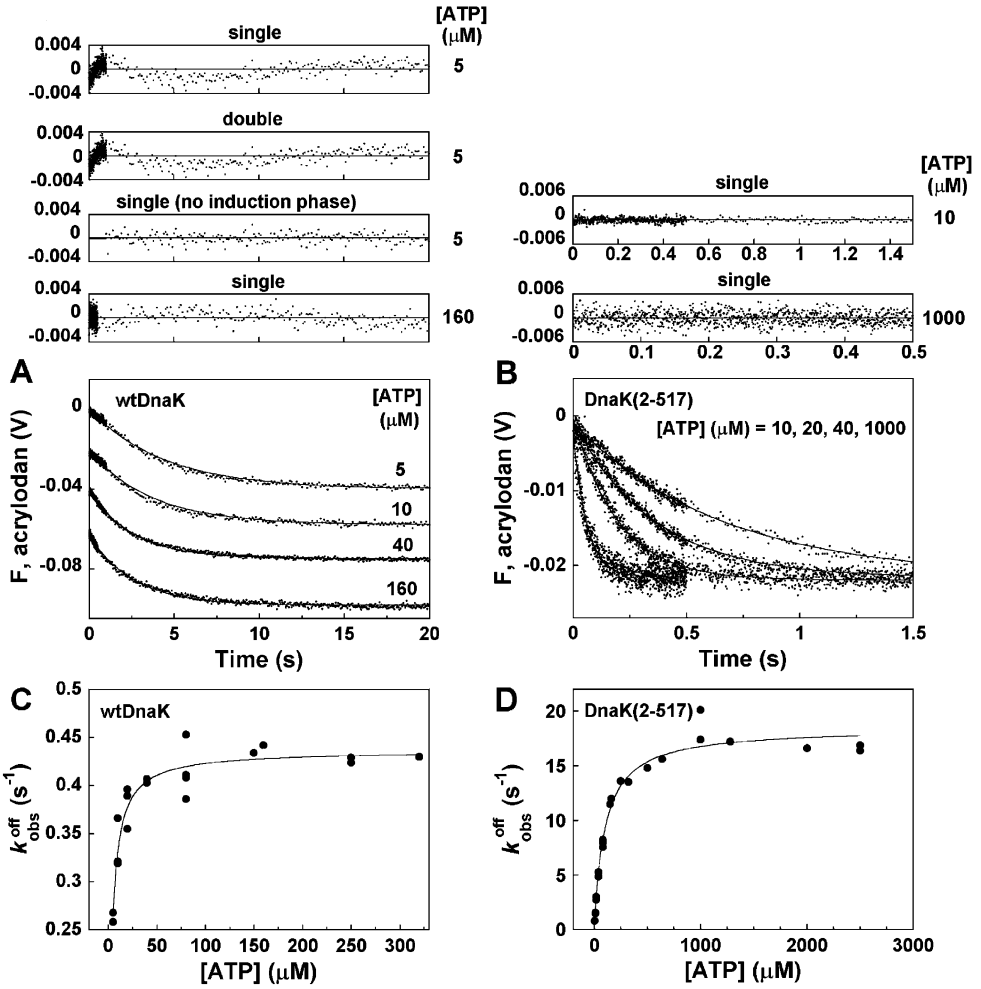

FIGURE 2: Kinetics of ap5 peptide dissociation from preformed DnaK·ap5 complexes triggered by ATP binding. (A) ap5 dissociation from wtDnaK. (B) ap5 dissociation from DnaK(2−517). For each protein, traces are fit to a single-exponential function, eq 4 (solid lines), yielding values for k^{off}_{obs}. Residuals, discussed in the text, are shown above panels A and B. Conditions: The reagents in the two stopped-flow syringes are shown in brackets, [wtDnaK or DnaK(2−517) + ap5] + [ATP + p5]. Concentrations after mixing were 1 μM protein, 0.05 μM ap5, 5 μM p5, 2.5−2500 μM ATP, and 5 mM (A) or 20 mM (B) $MgCl_2$. The excitation wavelength was 370 nm, and a 470 nm long pass filter was used to collect emission. Temperature = 5 °C. For clarity, traces in panel A are offset from each other by 0.01 V. Panels C and D show plots of k^{off}_{obs}(5 °C) vs [ATP] for dissociation data collected from wtDnaK and DnaK(2−517), respectively. Data are fit to $k^{off}_{obs} = k_2[ATP]/(K_{app} + [ATP])$ (solid lines). Parameters: wtDnaK, $k_2 = 0.44 \pm 0.01$ s^{-1} and $K_{app} = 3.2 \pm 0.4$ μM ($R = 0.953$). DnaK(2−517), $k_2 = 18.4 \pm 0.2$ s^{-1} and $K_{app} = 100 \pm 10$ μM ($R = 0.989$).

Table 1: Kinetic Parameters for the Forward and Reverse Reactions that Use the p5 Peptide[a]

Forward Reaction: $ATP + DnaK{\cdot}ap5 \overset{K_{app}}{\rightleftharpoons} ATP{\cdot}DnaK{\cdot}ap5 \xrightarrow{k_2} ATP{\cdot}DnaK + ap5^*$

Reverse Reaction: $p5 + ATP{\cdot}DnaK^* \underset{k_2}{\overset{k_{-2}}{\rightleftharpoons}} ATP{\cdot}DnaK{\cdot}p5$

	forward			reverse			ATPase
T (°C)	K_{app} (μM)	k_2 (s^{-1})	$k^a = (k_2/K_{app})$ ($M^{-1}s^{-1}$)	k_2 (s^{-1})	k_{-2} ($M^{-1}s^{-1}$)	k_2/k_{-2} (μM)	K_A (μM)
			wtDnaK				
5	3.2 ± 0.4	0.44 ± 0.1	$1.4 \pm 0.4 \times 10^5$	0.76 ± 0.51	$1.5 \pm 0.1 \times 10^5$	5.1 ± 3.8	4.5 ± 2.2
15	7.3 ± 1	2.0 ± 0.4	$2.7 \pm 0.7 \times 10^5$	2.4 ± 0.8	$3.4 \pm 0.1 \times 10^5$	7.1 ± 2.6	
25	28 ± 2	7.6 ± 0.5	$2.7 \pm 0.3 \times 10^5$	7.0 ± 3.1	$9.4 \pm 0.4 \times 10^5$	7.4 ± 3.8	
			DnaK(2−517)				
5	100 ± 10	18.4 ± 2	$1.8 \pm 0.3 \times 10^5$	20.4 ± 4.5	$2.8 \pm 0.3 \times 10^5$	73 ± 27	87 ± 20
15	289 ± 30	84 ± 4	$2.9 \pm 0.3 \times 10^5$	100 ± 7	$4.5 \pm 0.4 \times 10^5$	222 ± 33	
25	1060 ± 185	299 ± 21	$2.8 \pm 0.5 \times 10^5$				

[a] a = acrylodan.

Reverse Reaction: Peptide Binding to ATP-Bound DnaK Followed by Changes in Tryptophan Fluorescence. In this section, we focus on the reverse reaction, that is, p5 + ATP·DnaK* ⇌ ATP·DnaK·peptide. It was previously shown that a rapid burst of tryptophan fluorescence is observed upon mixing unlabeled peptide with ATP-bound wtDnaK and that

Table 2: Kinetic Parameters for the Forward and Reverse Reactions that Use the NR Peptide[a]

Forward Reaction: $ATP + DnaK{\cdot}fNR \overset{K_{app}}{\rightleftharpoons} ATP{\cdot}DnaK{\cdot}fNR \xrightarrow{k_2} ATP{\cdot}DnaK + fNR^*$

Reverse Reaction: $NR + ATP{\cdot}DnaK^* \underset{k_2}{\overset{k_{-2}}{\rightleftharpoons}} ATP{\cdot}DnaK{\cdot}NR$

	forward			reverse			ATPase
T (°C)	K_{app} (μM)	k_2 (s^{-1})	$k^a = (k_2/K_{app})$ ($M^{-1}s^{-1}$)	k_2 (s^{-1})	k_{-2} ($M^{-1}s^{-1}$)	k_2/k_{-2} (μM)	K_A (μM)
			wtDnaK				
5	1.3 ± 0.2	0.19 ± 0.03	$1.5 \pm 0.3 \times 10^5$	0.48 ± 0.03	$1.5 \pm 0.2 \times 10^4$	32 ± 2	29 ± 15
15	5.9 ± 0.6	1.1 ± 0.2	$1.9 \pm 0.4 \times 10^5$	2.1 ± 0.1	$4.8 \pm 0.2 \times 10^4$	44 ± 4	
25	25 ± 2	4.8 ± 0.3	$1.9 \pm 0.2 \times 10^5$	9.4 ± 1.0	$1.1 \pm 0.1 \times 10^5$	86 ± 6	
			DnaK(2−517)				
5	298 ± 35	32 ± 5	$1.1 \pm 0.2 \times 10^5$	32 ± 9	$2.2 \pm 0.5 \times 10^4$	1455 ± 950	
15	740 ± 105	150 ± 15	$2.0 \pm 0.4 \times 10^5$				
25	2260 ± 220	474 ± 30	$2.1 \pm 0.2 \times 10^5$				

[a] f = dansyl group.

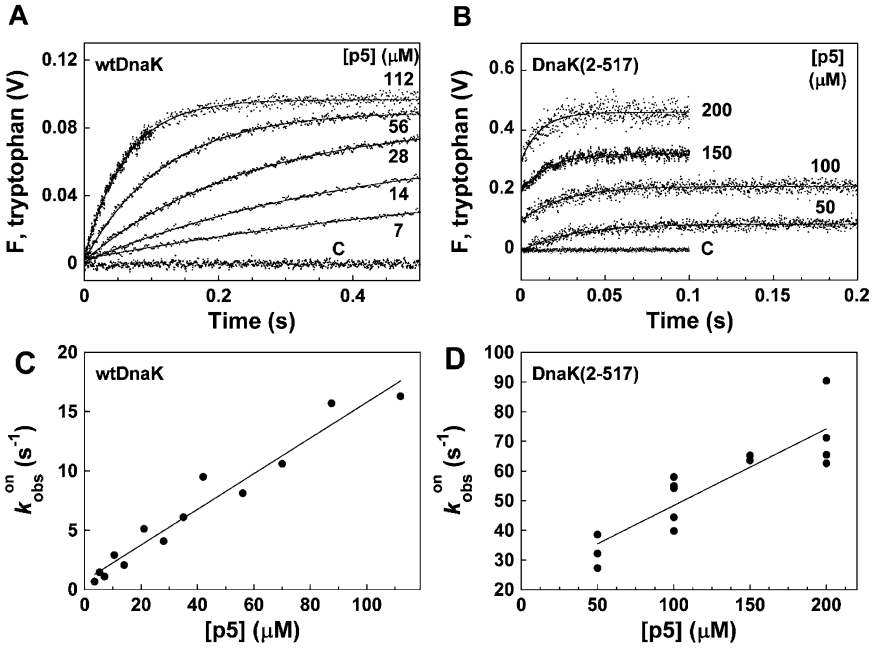

FIGURE 3: Kinetics of p5 binding to low affinity DnaK followed by changes in tryptophan fluorescence. (A) p5 + ATP·wtDnaK. As a negative control, wtDnaK (2 μM) was mixed with poly-glutamic acid (400 μM) (trace C). (B) p5 + ATP·DnaK(2−517). For wtDnaK and DnaK(2−517), traces are fit to a single-exponential function, eq 7 (solid lines), yielding values for k^{on}_{obs}. Conditions: The reagents in the two stopped-flow syringes are shown in brackets, [wtDnaK or DnaK(2−517) + ATP] + [ATP + p5]. Concentrations after mixing were (A) 1 μM protein, 7−200 μM p5, 1 mM ATP, and 5 mM $MgCl_2$ and (B) 8 mM ATP and 20 mM $MgCl_2$. The excitation wavelength was 295 nm, and a 320 nm long pass filter was used to collect emission. Temperature = 5 °C. For clarity, traces in panel B are offset from each other by 0.1 V. Panels C and D show plots of k^{on}_{obs} (5 °C) vs [ATP] for p5 peptide binding data collected from wtDnaK and DnaK(2−517), respectively. Data are fit to the equation $k^{on}_{obs} = k_{-2}[p5] + k_2$ (solid line), yielding $k_{-2} = 1.5 \pm 0.1 \times 10^5$ M^{-1} s^{-1} and $k_2 = 0.76 \pm 0.51$ s^{-1} ($R = 0.975$) for the wild-type protein (C), and $k_{-2} = 2.8 \pm 0.3 \times 10^5$ M^{-1} s^{-1} and $k_2 = 20.4 \pm 4.5$ s^{-1} ($R = 0.940$) for DnaK(2−517) (D).

this peptide-induced increase in tryptophan fluorescence occurs much faster than DnaK-mediated ATP hydrolysis (*17*). The question is, how does loss of the lid affect the reverse reaction? If the lid is rotated away from the exposed peptide-binding site in the ATP-bound form of the wild-type protein giving relatively unhindered access to entering peptides (*8*), then we hypothesize that deletion of the lid should not significantly improve the accessibility of the peptide-binding site, and thus it is predicted that the magnitude of k_{-2} should be similar for both proteins, i.e., k_{-2}(wtDnaK) ≈ k_{-2}(DnaK[2−517]).

The complex formation kinetic experiments were conducted under pseudo-first-order conditions ([p5] ≫ [ATP·DnaK*] or [ATP·DnaK(2−517)]), where the p5 peptide concentration was varied while maintaining a fixed concentration of the ATP-bound protein (1 μM). Representative formation traces, obtained at 5 °C, are shown in Figure 3A,B. Traces were fit to a single-exponential function (eq 7), yielding values for the observed first-order on-rate constant (k^{on}_{obs}). Trace "C" in panel A is a negative control. 400 μM poly-glutamic acid was mixed with an equal volume of ATP-bound wtDnaK. The lack of signal upon mixing is consistent with a lack of binding of poly-glutamic acid to ATP-bound DnaK. Thus, the increase in tryptophan fluorescence observed upon mixing with the p5 or NR peptide is a consequence of specific binding. Trace "C" in panel B is

Table 3: Comparison of Peptide On and Off Rates Constants for the Reaction P + ATP·DnaK* ⇌ ATP·DnaK·P[a]

T (°C)	reaction	k_2 (s^{-1})	k_{-2} (M^{-1} s^{-1})
5	p5 + ATP·DnaK(2−517) (Trp fluorescence)	20.4 ± 4.5	$2.8 \pm 0.3 \times 10^5$
5	ap5 + ATP·DnaK(2−517) (acrylodan fluorescence)	9.6 ± 0.4	$1.2 \pm 0.1 \times 10^5$
25	p5 + ATP·DnaK (Trp fluorescence)	7.0 ± 3.1	$9.4 \pm 0.4 \times 10^5$
25	ap5 + ATP·DnaK (acrylodan fluorescence)	4.5 ± 1.3	$1.1 \pm 0.1 \times 10^6$
25	ap5 + ATP·DnaK (acrylodan fluorescence)[b]	5.7	1.1×10^6
25	NR + ATP·DnaK (Trp fluorescence)	9.4 ± 1.3	$1.1 \pm 0.1 \times 10^5$
25	aNR + ATP·DnaK (acrylodan fluorescence)[b]	4.5	1.0×10^5

[a] Rate constants were determined by following increases in either the tryptophan fluorescence of dnak or the acrylodan fluorescence of the acrylodan-labeled peptide. [b] Data taken from Gisler et al. (*25*). a = acrylodan.

the output signal obtained on mixing nucleotide-free DnaK-(2−517) (2 μM) with an equal volume of p5 peptide (400 μM). Added peptide does not change the tryptophan fluorescence of nucleotide-free DnaK(2−517). Note that at 25 °C peptide binding to ATP·DnaK(2−517) molecules was too fast ($k_{obs}^{on} > 500$ s^{-1}) to be precisely measured with the stopped-flow instrument.

Figure 3C,D shows that k_{obs}^{on} values for the wild type protein and its lidless variant increase linearly with increasing concentrations of the p5 peptide. The linear plots are consistent with the reaction p5 + ATP·DnaK* ⇌ ATP·DnaK·P. The slope and *y*-intercept of the plots give values for k_{-2} and k_2, respectively. From the experiments conducted at 5 °C, k_{-2} and k_2 equal $1.5 \pm 0.1 \times 10^5$ M^{-1} s^{-1} and 0.76 ± 0.51 s^{-1}, respectively, for p5 binding to wtDnaK, whereas k_{-2} and k_2 equal $2.8 \pm 0.3 \times 10^5$ M^{-1} s^{-1} and 20.4 ± 4.5 s^{-1}, respectively, for p5 binding to DnaK(2−517). As expected, deletion of DnaK's lid does not significantly alter k_{-2}. Rate constants for p5 peptide binding to ATP·wtDnaK at other temperatures are given in Table 1. Notice that values for k_2, determined from the forward experiments, agree quite well with the values determined from the reverse experiments (Table 1). For comparison, the rate constants for the reverse reaction involving the NR peptide are given in Table 2.

Reverse Reaction: Peptide Binding to ATP-Bound DnaK Followed Changes in Acrylodan-Labeled Peptide Fluorescence. As indicated above, peptide binding to the C-terminal domain of ATP-bound DnaK triggers a concerted conformational change in the N-terminal domain that quenches the fluorescence of Trp^{102}. If the kinetic constants derived from such experiments are accurate, the same rate constants should be obtained when changes in the fluorescence of a labeled peptide are measured. Because the reaction between ATP-bound wtDnaK and the ap5 peptide at 25 °C has been studied in detail (*25*), this reaction was studied.

DnaK-fluorescent peptide complex formation experiments were conducted under pseudo-first-order conditions ([ATP·DnaK*] ≫ [ap5]), where the concentration of ATP-bound wtDnaK was varied while maintaining a fixed concentration of ap5 (0.05 μM). The complex formation traces are shown in Figure 4A. Traces were fit to a single-exponential function (eq 7), yielding values for k_{obs}^{on}. Consistent with what is expected for a ligand binding to and releasing from a protein, k_{obs}^{on} values increase linearly with increasing concentrations of ATP-bound DnaK (Figure 4B). The slope and *y*-intercept of the plot of k_{obs}^{on} versus [wtDnaK] equal k_{-2} ($1.1 \pm 0.1 \times 10^6$ M^{-1} s^{-1}) and k_2 (4.5 ± 1.3 s^{-1}), respectively. These rate

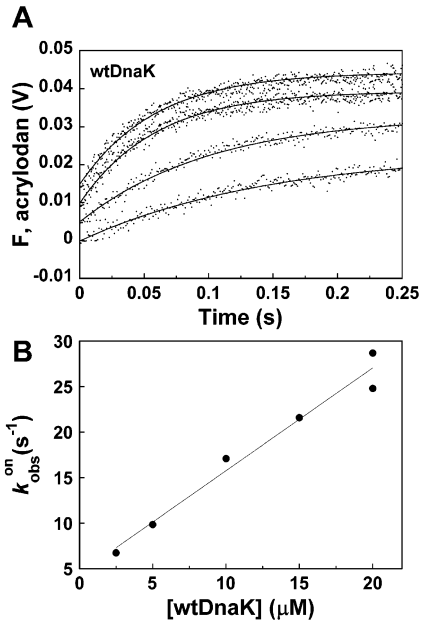

FIGURE 4: Kinetics of ap5 binding to ATP-bound wtDnaK followed by changes in acrylodan fluorscence. (A) ap5 + ATP·wtDnaK. Traces are fit to a single-exponential function, eq 4 (solid lines), yielding values for k_{obs}^{on}. Starting from the top trace, [wtDnaK] = 20, 15, 10, and 5 μM. (B) Plot of k_{obs}^{on} vs [wtDnaK]. Data are fit to the equation $k_{obs}^{on} = k_{-2}$[wtDnaK] + k_2 (solid line), yielding $k_{-2} = 1.1 \pm 0.1 \times 10^6$ M^{-1} s^{-1} and $k_2 = 4.5 \pm 1.3$ s^{-1} ($R = 0.986$). Conditions: The reagents in the two stopped-flow syringes are shown in brackets, [wtDnaK + ATP] + [ap5 + ATP]. Concentrations after mixing were 0.05 μM ap5, 1 mM ATP, and 2.5−20 μM ATP·wtDnaK. The excitation wavelength was 370 nm, and a 470 nm long pass filter was used to collect emission. Temperature = 25 °C. Traces are offset from each other by 0.005 V.

constants agree with those determined by Gisler et al. (*25*) (Table 3). Moreover, these rate constants are identical within the experimental error to those determined from the experiments that monitored the p5-induced increase in DnaK's tryptophan fluorescence (Table 3). This is a key finding: experiments that monitor peptide-induced changes in DnaK's tryptophan fluorescence give the same results as those that monitor DnaK-induced changes in labeled-peptide fluorescence.

Steady-State ATPase Assay. Apparent rate constants for peptide binding to and release from ATP-bound DnaK were determined using two different fluorescence assays. Another way to probe this reaction is to measure the steady-state ATPase activity of DnaK at different concentrations of added peptide. Plots of k_{cat} versus [peptide] are hyperbolic, and the concentration of peptide (K_A) that gives half-maximal

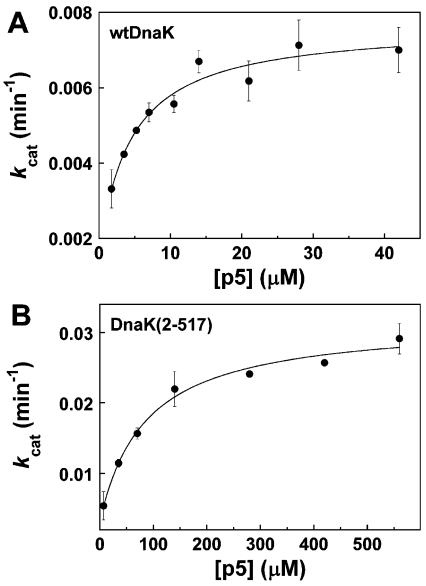

FIGURE 5: Plots of k_{cat} vs p5 concentration. (A) Wild-type DnaK. A least-squares fit of the data to the equation $y = c + k_{cat}^{max}[p5]/(K_A + [p5])$ (solid line) yields c, k_{cat}^{max}, and K_A equal to 0.0016 ± 0.0010 min^{-1}, 0.0061 ± 0.0008 min^{-1}, and 4.5 ± 2.2 μM, respectively ($R = 0.977$). (B) DnaK(2−517). A least-squares fit of the data to the above equation (solid line) yields c, k_{cat}^{max}, and K_A equal to 0.0033 ± 0.0016 min^{-1}, 0.028 ± 0.002 min^{-1}, and 87 ± 20 μM, respectively ($R = 0.991$). Temperature = 5 °C.

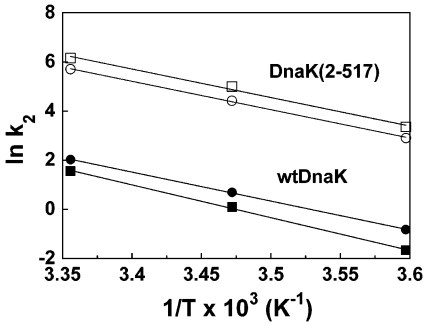

FIGURE 6: Arrhenius plots. Values for k_2 are from Tables 1 and 2. Solid lines are the linear least-squares fit of the data to the equation $\ln k_2 = \ln \omega + \Delta S^*/R - \Delta H^*/RT$. ●, p5/wtDnaK: $\Delta H^* = 23.4 \pm 1.3$ kcal mol^{-1} and frequency factor = $1.2 \times 10^{18\pm1}$ s^{-1} (R=0.994). ○, p5/DnaK(2−517): $\Delta H^* = 23.0 \pm 0.8$ kcal mol^{-1} and frequency factor = $2.1 \times 10^{19\pm0.6}$ s^{-1} ($R = 0.998$). ■, NR/wtDnaK: $\Delta H^* = 26.6 \pm 1.5$ kcal mol^{-1} and frequency factor = $1.8 \times 10^{20\pm1}$ s^{-1} ($R = 0.994$). □, NR/DnaK(2−517): $\Delta H^* = 22.3 \pm 1.4$ kcal mol^{-1} and frequency factor = $1.1 \times 10^{19\pm1}$ s^{-1} ($R = 0.993$). Error bars are of the same size as the symbols.

response can be thought of as the equilibrium dissociation constant for the reaction ATP·DnaK·p5 ⇌ ATP·DnaK* + p5 (*31*). K_A values from such experiments should equal k_2/k_{-2} (Table 1).

Panels A and B of Figure 5 show plots of k_{cat} versus the concentration of p5 peptide for wtDnaK and DnaK(2−517), respectively. K_A values for p5-stimulated ATP hydrolysis mediated by wtDnaK and DnaK(2−517) at 5 °C are 4.5 ± 2.2 and 87 ± 20 μM, respectively. Comparing this to the results in Table 1, we see that K_A for wtDnaK and DnaK(2−517) in the presence of ATP at 5 °C k_2/k_{-2} equals 5.1 ± 3.8 and 73 ± 27 μM, respectively. The agreement between these two very different assays supports peptide binding to ATP-bound DnaK via reaction 1.

Table 4: Activation Parameters

dissociation parameter	ΔH^* (kcal mol^{-1})	$\omega \exp(\Delta S^*/R)$ (s^{-1})
k_2 (ap5/wtDnaK)	23.4 ± 1.3	$1.2 \times 10^{18\pm1}$
k_2 (ap5/DnaK[2−517])	23.0 ± 0.8	$2.1 \times 10^{19\pm0.6}$
k_2 (fNR/wtDnaK)	26.6 ± 1.5	$1.8 \times 10^{20\pm1}$
k_2 (fNR/DnaK[2−517])	22.3 ± 1.4	$1.1 \times 10^{19\pm1}$
association parameter[a]	ΔH^* (kcal mol^{-1})	$\omega \exp(\Delta S^*/R)$ (M^{-1} s^{-1})
k_{-2} (p5+wtDnaK)	14.5 ± 0.8	$1.3 \times 10^{14\pm0.6}$
k_{-2} (NR+wtDnaK)	15.9 ± 1.2	$1.8 \times 10^{14\pm0.9}$

[a] The enthalpy and frequency prefactor for association were determined from a plot of ln(k_{-2}/T) vs 1/T.

Activation Parameters. We have previously reported that many of the reactions between DnaK and peptides, whether binding or dissociation, are characterized by unusually large activation enthalpies when the reactions are carried out with ADP and that, in general, the presence of ATP lowers these activation enthalpy barriers (*32*, *33*). To ascertain how loss of the lid affects the activation barriers, the temperature dependence of k_2 and k_{-2} was examined. Arrhenius plots of the parameter k_2, determined from the forward experiments (Tables 1 and 2), are shown in Figure 6. The activation enthalpy (ΔH^*) and frequency prefactor ($\omega \exp[\Delta S^*/R]$) are determined form the slope and y-intercept of the plots, respectively. The upper plots are for peptide dissociation from DnaK(2−517), whereas the lower plots are for peptide dissociation from wtDnaK. The activation parameters for k_2 and k_{-2} are given in Table 4. The thermodynamic parameters are discussed below.

DISCUSSION

The following evidence supports a two-step mechanism (eq 1) for the interaction of DnaK(2−517) with ATP and added peptide: (i) Analysis of the forward reaction, peptide dissociation, yields the rate constant k_2. When the reverse reaction is studied, the same k_2 value is obtained from the y-intercept of plot of k_{obs}^{on} versus [peptide] (Tables 1 and 2). (ii) Analysis of the reverse reaction, whether studied by monitoring the intrinsic fluorescence of the protein or of the labeled peptide, yields the same values for the rate constants k_2 and k_{-2} (Figures 3 and 4; Table 3). (iii) The apparent equilibrium dissociation constant, K_A, obtained from the ATPase experiments, equals k_2/k_{-2} (Figure 5; Tables 1 and 2). These findings support a model in which peptide binding to the ATP·DnaK* state triggers a very rapid and concerted conformational change in the ATPase domain that quenches the fluorescence of Trp^{102} and the fact that this peptide-triggered conformational change occurs before ATP hydrolysis.

The striking findings in this study are revealed by comparing results obtained at 15 °C for wtDnaK and DnaK(2−517):

$$\text{ATP} + \text{wtDnaK·p5} \overset{7.3\ \mu\text{M}}{\rightleftharpoons} \text{ATP·wtDnaK·p5} \underset{3.4 \times 10^5\ \text{M}^{-1}\ \text{s}^{-1}}{\overset{2.4\ \text{s}^{-1}}{\rightleftharpoons}} \text{ATP·wtDnaK*} + \text{p5} \quad (10)$$

Our interpretation of these reactions, and the other results

$$\text{ATP} + \text{DnaK}(2-517)\cdot\text{p5} \overset{289\ \mu\text{M}}{\rightleftharpoons} \text{ATP}\cdot\text{DnaK}(2-517)\cdot\text{p5} \overset{90\ \text{s}^{-1}}{\underset{4.5\times10^5\ \text{M}^{-1}\ \text{s}^{-1}}{\rightleftharpoons}} \text{ATP}\cdot\text{DnaK}(2-517)^* + \text{p5} \quad (11)$$

in this study, is that the lid is a cis-acting structural component that down-regulates the rate of interdomain communication in DnaK. By reducing the rate of the forward conformational change, k_2, the lid increases the affinity of substrates for ATP·DnaK. The key questions are, why does loss of the lid appear to affect ATP binding (K_{app}) and how does the lid retard the rate of the ATP-triggered conformational change?

Regarding the first question, we found that, at a given temperature, deletion of the lid increases k_2 and K_{app} by about the same amount (compared to wild type). This can be seen from the data in Table 5 at a given temperature

$$\frac{K_{app}(\text{L})}{K_{app}(\text{WT})} \approx \frac{k_2(\text{L})}{k_2(\text{WT})}$$

where L and WT refer to DnaK(2−517) and wtDnaK, respectively. Thus, empirically, the increase in K_{app} upon deletion of the lid is due to the increase in k_2. It is easy to see why this is true, given that

$$K_{app} = \frac{k_{-1}^{ATP} + k_2}{k_1^{ATP}}.$$

For DnaK(2−517), given the large values for k_2, a reasonable assumption is that $k_2 \gg k_{-1}$, thus

$$K_{app}(\text{L}) \approx \frac{k_2(\text{L})}{k_1^{ATP}}$$

Similarly, for the wild-type protein, if $k_2 > k_{-1}$, then

$$K_{app}(\text{WT}) \approx \frac{k_2(\text{WT})}{k_1^{ATP}}$$

Our interpretation of these results is that the loss of the lid has no appreciable effect on the conformation of the ATPase domain; the increase in K_{app} upon loss of the lid is due to the increase in k_2.

In the nucleotide-free and ADP-bound states of DnaK, the lid is thought to be attached to the β-sandwich domain via a network of noncovalent interactions, referred to as the latch (Figure 1). A consequence of this attachment, we propose, is that the lid (l) constrains motions and rearrangements of the β-sandwich (β) that occur following ATP binding. In terms of a chemical equation, we propose that for the wild-type protein, ATP triggers peptide release at 25 °C according to

$$\text{ATP} + \text{E}\beta_c\text{l}_c\cdot\text{P} \overset{K_{-1}}{\rightleftharpoons} \text{ATP}\cdot\text{E}\beta_c\text{l}_c\cdot\text{P} \xrightarrow{k_2 = 2-8\ \text{s}^{-1}} \text{ATP}\cdot\text{E}^*\beta_o\text{l}_o + \text{P} \quad (12)$$

where $\text{E}\beta_c\text{l}_c\cdot\text{P}$ is the high-affinity wtDnaK−peptide complex in which both the β-sandwich and lid are closed, $\text{ATP}\cdot\text{E}\beta_c\text{l}_c\cdot$P is an intermediate from which ATP hydrolysis is likely to occur (*11*), $\text{ATP}\cdot\text{E}\beta_o\text{l}_o$ is the low-affinity state in which both the β-sandwich and lid subdomains are open, and the asterisk indicates reduced tryptophan fluorescence. Deletion of the lid eliminates the constraints on the motions of the β-sandwich, which, upon ATP binding, occur with a characteristic rate constant between 300 and 470 s^{-1} at 25 °C (Tables 1 and 2), and peptide releases according to

Table 5: Comparison of changes in k_2 and K_{app}

	p5 peptide		NR peptide	
T (°C)	k_2(L)/k_2(WT)	K_{app}(L)/K_{app}(WT)	k_2(L)/k_2(WT)	K_{app}(L)/K_{app}(WT)
5	42 ± 5	31 ± 5	168 ± 37	229 ± 44
15	49 ± 9	40 ± 7	136 ± 28	125 ± 22
25	39 ± 4	38 ± 12	99 ± 9	90 ± 11

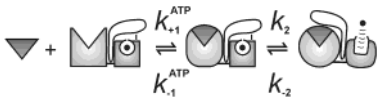

FIGURE 7: Proposed model for the lid as a cis-acting down regulator of the ATP-triggered conformational change. The inverted triangle represents ATP. The black circle is a bound peptide.

$$\text{ATP} + \text{E}\beta_c\cdot\text{P} \overset{K_{-1}}{\rightleftharpoons} \text{ATP}\cdot\text{E}\beta_c\cdot\text{P} \xrightarrow{k'_2 = 300-470\ \text{s}^{-1}} \text{ATP}\cdot\text{E}^*\beta_o + \text{P} \quad (13)$$

The fact that ATP-triggers fNR peptide dissociation from nucleotide-free DnaK(2−517) with k_{obs}^{off} equal to 474 s^{-1} at 25 °C (Table 2), whereas the fNR peptide dissociates from ADP-bound clDnaK(1−517)[2] with k_{obs}^{off} equal to 0.1 s^{-1} (*17*), is strong evidence that the β-sandwich can exist in either a closed or open conformation. One way to test this model is to engineer a DnaK variant that lacks the network of hydrogen bonds and the salt bridge that comprise the latch. The model predicts very rapid peptide dissociation from such a full-length DnaK variant ($k_{obs}^{off} \approx 300-470\ \text{s}^{-1}$). A schematic of this proposed model is shown in Figure 7.

Notice that concerted motions of the β-sandwich and lid occur in the second step of reaction 12. Of course, one can envision that the lid and β-sandwich are independent (*17*) and that their respective motions occur sequentially

$$\text{ATP} + \text{E}\beta_c\text{l}_c\cdot\text{P} \underset{k_{-1}^{ATP}}{\overset{k_1^{ATP}}{\rightleftharpoons}} \text{ATP}\cdot\text{E}\beta_c\text{l}_c\cdot\text{P} \overset{k_{lco}}{\underset{k_{loc}}{\rightleftharpoons}} \text{ATP}\cdot\text{E}\beta_c\text{l}_o\cdot\text{P} \overset{k_{\beta co}}{\underset{k_{\beta oc}}{\rightleftharpoons}} \text{ATP}\cdot\text{E}^*\beta_o\text{l}_o + \text{P} \quad (14)$$

In the above reaction, lid opening (k_{lco}) occurs at 2−8 s^{-1} and is the rate-limiting step for peptide dissociation (*25*). Upon deletion of the lid peptide, dissociation is governed by the opening of the β-sandwich ($k_{\beta co}$); therefore, the maximal rate of peptide dissociation jumps from 2−8 to 300−470 s^{-1}. This three-step mechanism cannot be ruled out. However, because the ATPase and β-sandwich domains are connected, ATP binding most certainly triggers a conformational change first in the β-sandwich domain, rather than in the lid, as indicated in reaction 12. For this reason, we favor reaction 12, where the lid, like a mechanical

[2] clDnaK(1−517) is prepared by tryptic cleavage of an N-terminal GST tag from DnaK(1−517). Ten residues remain attached at the N-terminus of DnaK(1−517) after cleavage, and this is denoted by "cl".

governor, impedes motions of the β-sandwich. In addition, to date there is no evidence for this third step.

We have now analyzed the kinetics of three different peptides binding to ATP-bound wtDnaK. It is interesting to compare the k_{-2} values of these different peptides. Cro, NR, and the p5 peptides bind to ATP-bound wtDnaK at 25 °C, with k_{-2} equal to 2.4×10^4 (*11*), 1.1×10^5, and 9.4×10^5 M^{-1} s^{-1}. These rate constants are much less than the rate constant for a diffusion controlled reaction, which for an enzyme−substrate interactions occur at $\sim 10^9$ $M^{-1}s^{-1}$. Despite the sequence and charge differences among these peptides, for each peptide, the activation enthalpy equals 15 kcal mol^{-1} for the reaction, peptide + ATP−DnaK* → ATP−DnaK−peptide. This suggests that entropic effects play a significant role in peptide binding to ATP-bound DnaK. Perhaps the peptide must adopt a precise conformation in order to be captured.

Physiological Relevance. In vivo experiments have shown that the related protein, DnaK(2−507), supports the propagation of bacteriophage λ, albeit at about 25% of the efficiency as the wild-type protein (*15*). Other in vivo experiments showed that the *dnaK163* allele, which encodes for DnaK(2−538), complements the temperature-sensitive phenotype observed in the *E. coli* strain BB1553, which is a DnaK null strain, only at very high concentrations of IPTG (*16*). Our view is that these lidless forms of DnaK, be it DnaK(2−507) or DnaK(2−517) or DnaK(2−538), are defective proteins compared to wild type. They are defective because the rate constant for substrate release is huge, falling in the range of 300−475 s^{-1} at 25 °C, which means that these three lidless forms of DnaK bind to substrates with very low affinities. For example, at 15 °C, the p5 peptide binds to DnaK(2−517) with an apparent K_d equal to 222 μM (Table 1), whereas for the wild-type protein, $K_d = 7.1$ μM. Of course, the intrinsically low affinity of these lidless forms for substrates may be compensated for thermodynamically by overexpressing the variants in cells via induction with IPTG. This explains why Mayer and co-workers found that at relatively low concentrations DnaK(2−538) (0.5 μM) cannot refold luciferase in an in vitro folding assay, whereas overexpression of DnaK(2−538) in vivo compensates for the temperature sensitive phenotype of BB1553.

In summary, the importance of the lid is illustrated by using the activation parameters in Table 4 to estimate values for the rate of peptide dissociation (k_2) at, say, 42 °C. For ATP-triggered dissociation of ap5 from wild type and DnaK(2−517), k_2 equals 70 and 2300 s^{-1}, respectively. For ATP-triggered fNR dissociation from wild type and DnaK(2−517), k_2 equals 63 and 3700 s^{-1}, respectively. Without the lid, ATP-bound DnaK has incredibly weak affinity for the p5 or the NR peptide at this elevated temperature. Loss of the lid probably also reduces peptide affinity for DnaK in the absence of ATP because, for the NR peptide, loss of the lid (residues 518−638) results in 10- and 100-fold increases in the peptide on and off rates, respectively, for experiments conducted in the presence of excess ADP (*17*).

ACKNOWLEDGMENT

We thank Michael Sehorn for conducting an initial characterization of DnaK(2-517), for helping with figures, and for a critical reading of the manuscript.

APPENDIX

As mentioned in the Introduction, suppose the second step of two-step reaction 1 is composed of two distinct steps, according to

$$\mathrm{ATP} + \mathrm{DnaK{\cdot}P} \underset{k_{-1}^{\mathrm{ATP}}}{\overset{k_1^{\mathrm{ATP}}}{\rightleftharpoons}} \mathrm{ATP{\cdot}DnaK{\cdot}P} \underset{k_{-2}}{\overset{k_2}{\rightleftharpoons}} \mathrm{ATP{\cdot}DnaK^*{\cdot}P} \underset{k_{-3}}{\overset{k_3}{\rightleftharpoons}} \mathrm{ATP{\cdot}DnaK^*} + \mathrm{P} \quad (15)$$

ATP binding, a conformational change, and peptide release occur sequentially, and the asterisk denotes a state with reduced fluorescence relative to the DnaK·P state. Notice that whether the above reaction is carried out in the forward or reverse directions, the change in fluorescence occurs in the second step. Previous simulations of this reaction (*11*), which explored a very limited parameter space, yielded simulated traces that did not mimic experimental traces. The specific parameters used in these simulations were as follows: $k_{-1}^{\mathrm{ATP}}/k_1^{\mathrm{ATP}} = 22$ μM, $k_2 = 3$ s^{-1}, $k_{-2} = 0.1$ s^{-1}, $k_3 = 0.1$ or 30 s^{-1}, and $k_{-3} = 2 \times 10^4$ M^{-1} s^{-1}, with initial concentrations 1 μM DnaK·P, 20 − 400 μM peptide, and 500 μM ATP; the fluorescence factors were F(DnaK·P) = F(ATP·DnaK·P) = 1 and F(ATP·DnaK*·P) = F(ATP·DnaK*) = 0.85.

We have conducted new simulations of this three-step reaction, using the program KINSIM (*29*), and have found that when $k_2 \approx k_{-2}$ and $k_3 > k_2$ the simulated changes in protein fluorescence, for forward and reverse reactions, are quite similar to what is observed experimentally. These new simulations, and simulations of two-step reaction 1, are discussed below.

Reaction 16 was simulated in the forward and reverse directions. The forward reaction, ATP-triggered fluorescent peptide dissociation

$$\mathrm{ATP} + \mathrm{E{\cdot}P} \underset{7.5\ \mathrm{s^{-1}}}{\overset{270\,000\ \mathrm{M^{-1}s^{-1}}}{\rightleftharpoons}} \mathrm{ATP{\cdot}E{\cdot}P} \underset{5\ \mathrm{s^{-1}}}{\overset{5\ \mathrm{s^{-1}}}{\rightleftharpoons}} \mathrm{ATP{\cdot}E^*{\cdot}P} \underset{1.5\ \mathrm{million\ M^{-1}\ s^{-1}}}{\overset{50\ \mathrm{s^{-1}}}{\rightleftharpoons}} \mathrm{ATP{\cdot}E^*} + \mathrm{P} \quad (16)$$

was simulated with initial concentrations of [E·P] = 1 μM and [ATP·E·P] = [ATP·E*·P] = [ATP·E*] = [P] = 0; no peptide rebinding was possible ($k_{-3} = 0$), and the peptide fluorescence factors were F(E·P) = F(ATP·E·P) = F(ATP·E*·P) = 1 and F(P) = 0.5. The reverse reaction, the peptide-triggered conformational change, was simulated with initial concentrations of [ATP·E*] = 1 μM, [E·P] = [ATP·E·P] = [ATP·E*·P] = 0, and [ATP] = 1 mM, and the protein fluorescence factors were F(E·P) = F(ATP·E·P) = 1 and F(ATP·E*·P) = F(ATP·E*) = 0.85. Simulated traces in each direction follow single-exponential kinetics (data not shown).

For the forward reaction, the plot of $k_{\mathrm{obs}}^{\mathrm{off}}$ versus [ATP] is hyperbolic (Figure 8A) and follows relation 17, which was obtained using the steady-state approximation:

$$k_{\mathrm{obs}}^{\mathrm{off}} = \frac{\dfrac{k_2 k_3}{2k_2 + k_3}[\mathrm{ATP}]}{K_{\mathrm{app}} + [\mathrm{ATP}]} \quad (17)$$

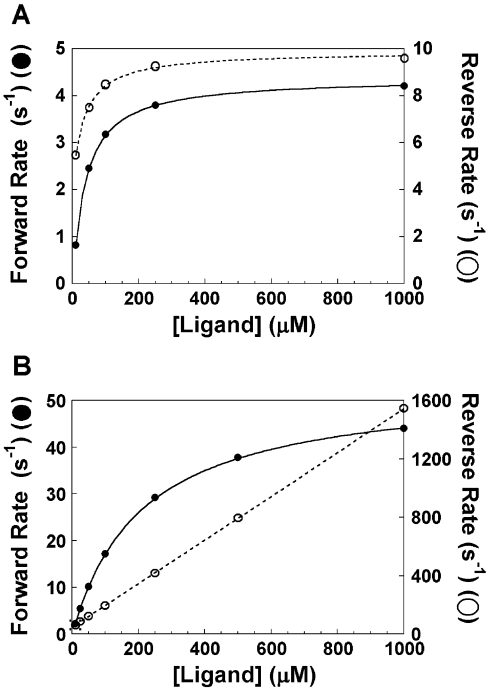

FIGURE 8: Simulations. (A) Three-step mechanism (eq 16). Apparent rate constants from the forward reaction (●) are fit to $k_{obs}^{off} = \{k_2k_3[ATP]/(2k_2 + k_3)\}/\{K_{app} + [ATP]\}$ (solid line), yielding $k_2k_3/(2k_2 + k_3) = 4.4\ s^{-1}$ and $K_{app} = 40.3\ \mu M$. Apparent rate constants from the reverse reaction (○) are fit to $k_{obs}^{on} = k_2 + k_{-2}[ATP]/(K_{app} + [ATP])$ (dashed line), yielding $k_2 + k_{-2} = 9.9\ s^{-1}$ and $K_{app} = 34.2\ \mu M$. (B) Two-step mechanism (eq 20). Apparent rate constants from the forward reaction (●) are fit to $k_{obs}^{off} = k_2[ATP]/(K_{app} + [ATP])$ (solid line), yielding $k_2 = 53\ s^{-1}$ and $K_{app} = 211\ \mu M$. Apparent rate constants from the reverse reaction (○) are fit to $k_{obs}^{on} = k_{-2}[P] + k_2$ (dashed line), yielding $k_{-2} = 1.5 \times 10^6\ M^{-1}\ s^{-1}$ and $k_2 = 47\ s^{-1}$. Parameters and conditions are given in the Appendix.

where K_{app} is defined by

$$K_{app} = \frac{k_{-1}k_2 + k_2^2 + k_{-1}k_3 + k_2k_3 - k_2k_{-2}}{k_1(2k_2 + k_3)} \quad (18)$$

In the case where $k_3 \gg k_2$, eq 17 simplifies to eq 5, with $K_{app} = (k_{-1}^{ATP} + k_2)/k_1^{ATP}$ and an asymptote equal to k_2. In this case, which is most applicable to DnaK, a three-step reaction is kinetically indistinguishable from a two-step reaction in which k_2 equals 5 s^{-1}.

For the reverse reaction, the plot of k_{obs}^{on} versus [peptide] is also hyperbolic (Figure 8A). The rate data obey the following relation, which was derived using the steady-state approximation

$$k_{obs}^{on} = k_2 + \frac{k_{-2}[P]}{\frac{k_{-2} + k_3}{k_{-3}} + [P]} \quad (19)$$

The asymptote of the plot ([P]→ ∞) is $k_2 + k_{-2}$ (= 10 s^{-1}). One reason that we favor two-step reaction 1 as the mechanism for DnaK is that, for three different peptides, we have never obtained a hyperbolic plot of k_{obs}^{on} versus [peptide]. Of course, possibly we have not gone to large enough concentrations of peptide; thus, the linear region of the hyperbolic plot was sampled. Because the Cro (MQERITLKDYAM) peptide is more soluble than either the NR or p5 peptides, we have extended our original experiments (*11*) of the reverse reaction out to 1.2 mM Cro, and the plot of k_{obs}^{on} versus [Cro] is still linear.

For comparison, reaction 20 was simulated in the forward and reverse directions:

$$ATP + E{\cdot}P \underset{7.5\ s^{-1}}{\overset{270\,000\ M^{-1}s^{-1}}{\rightleftharpoons}} ATP{\cdot}E{\cdot}P \underset{1.5\ \text{million}\ M^{-1}\ s^{-1}}{\overset{50\ s^{-1}}{\rightleftharpoons}} ATP{\cdot}E^* + P \quad (20)$$

The forward reaction was simulated with initial concentrations of [E·P] = 1 μM and [ATP·E·P] = [ATP·E*] = [P] = 0; no peptide rebinding was possible ($k_{-2} = 0$), and the peptide fluorescence factors were $F(E{\cdot}P) = F(ATP{\cdot}E{\cdot}P) = 1$ and $F(P) = 0.5$. The reverse reaction was simulated with initial concentrations of [ATP·E*] = 1 μM, [E·P] = [ATP·E·P] = 0, and [ATP] = 1 mM, and the protein fluorescence factors were $F(E{\cdot}P) = F(ATP{\cdot}E{\cdot}P) = 1$ and $F(ATP{\cdot}E^*) = 0.85$. Simulated traces in each direction follow single-exponential kinetics (data not shown). Plots of k_{obs} versus ligand concentration (ATP or peptide) are shown in Figure 8B.

The data from this and a previous study (*11*) are inconsistent with a three-step reaction in which $k_3 \gg k_2$, for the following reason. Consider the results for the reaction of the p5 peptide with wtDnaK. From the analysis of the forward reaction, the asymptote of the plot of k_{obs}^{off} versus [ATP] yields $k_2 = 0.45\ s^{-1}$ (Figure 2C). To have reversibility, three-step reaction 15 must have $k_2 \approx k_{-2}$. Thus, for the reverse reaction, the plot of k_{obs}^{on} versus [P] must have an asymptote ($= k_2 + k_{-2}$) equal to 1 s^{-1}. However, the plot of k_{obs}^{on} versus [p5] in Figure 3C is linear, with $k_{obs}^{on} = 15\ s^{-1}$ at 100 μM p5. If that plot ever reaches an asymptote, the value of the asymptote will be greater than 30 s^{-1}, which means that $k_{-2} \geq 30\ s^{-1}$. With values of $k_2 = 0.5$ and $k_{-2} \geq 30\ s^{-1}$, ATP binding to DnaK would not trigger a perceptible conformational change in DnaK.

REFERENCES

1. Bukau, B., and Horwich, A. L. (1998) *Cell 92*, 351−66.
2. Witt, S. N., and Slepenkov, S. V. (1999) *J. Fluorescence 9*, 281−93.
3. Ellis, R. J., and Hartl, F. U. (1999) *Curr. Opin. Struct. Biol. 9*, 102−10.
4. Agashe, V. R., and Hartl, F. U. (2000) *Semin. Cell Dev. Biol. 11*, 15−25.
5. Hartl, F. U., and Hayer-Hartl, M. (2002) *Science 295*, 1852−8.
6. Flaherty, K. M., DeLuca-Flaherty, C., and McKay, D. B. (1990) *Nature 346*, 623−28.
7. Morshauser, R. C., Wang, H., Glynn, G. C., and Zuiderweg, R. P. (1995) *Biochemistry 34*, 6261−66.
8. Zhu, X., Zhao, X., Burkholder, W. F., Gragerov, A., Ogata, C. M., Gottesman, M. E., and Hendrickson, W. A. (1996) *Science 272*, 1606−14.
9. Palleros, D. R., Reid, K. L., Shi, L., Welch, W. J., and Fink, A. L. (1993) *Nature 365*, 664−66.
10. Schmid, D., Baici, A., Gehring, H., and Christen, P. (1994) *Science 263*, 971−73.
11. Slepenkov, S. V., and Witt, S. N. (1998) *Biochemistry 37*, 16749−56.
12. Flynn, G. C., Chappell, T. G., and Rothman, J. E. (1989) *Science 245*, 385−90.
13. Sadis, S., and Hightower, L. E. (1992) *Biochemistry 31*, 9406−12.
14. Blond-Elguindi, S., Fourie, A. M., Sambrook, J. F., and Gething, M.-J. H. (1993) *J. Biol. Chem. 268*, 12730−35.

15. Pellecchia, M., Montgomery, D. L., Stevens, S. Y., Vander Kooi, C. W., Feng, H.-P., Gierasch, L. M., and Zuiderweg, E. R. P. (2000) *Nat. Struct. Biol. 7*, 298−303.
16. Mayer, M., Schroder, H., Rudiger, S., Paal, K., Laufen, T., and Bukau, B. (2000) *Nat. Struct. Biol. 7*, 586−93.
17. Buczynski, G., Slepenkov, S. V., Sehorn, M. G., and Witt, S. N. (2001) *J. Biol. Chem. 276*, 27231−36.
18. Theyssen, H., Schuster, H.-P., Packschies, L., Bukau, B., and Reinstein, J. (1996) *J. Mol. Biol. 263*, 657−70.
19. Slepenkov, S. V., and Witt, S. N. (1998) *Biochemistry 37*, 1015−24.
20. Bardwell, J. C. A., and Craig, E. A. (1984) *Proc. Natl. Acad. Sci. U.S.A. 81*, 848−52.
21. Russell, R., Jordan, R., and McMacken, R. (1998) *Biochemistry 37*, 596−607.
22. Gao, B., Greene, L., and Eisenberg, E. (1994) *Biochemistry 33*, 2048−54.
23. Bukau, B., and Walker, G. C. (1989) *J. Bacteriol. 171*, 6030−38.
24. Gragerov, A., Zeng, L., Zhao, X., Burkholder, W., and Gottesman, M. E. (1994) *J. Mol. Biol. 235*, 848−54.
25. Gisler, S. M., Pierpaoli, E. V., and Christen, P. (1998) *J. Mol. Biol. 279*, 833−40.
26. Pierpaoli, E. V., Sanmeier, E., Baici, A., Schönfeld, H.-J., Gisler, S., and Christen, P. (1997) *J. Mol. Biol. 269*, 757−68.
27. Sehorn, M. G., Slepenkov, S. V., and Witt, S. N. (2002) *Biochemistry 41*, 8499−507.
28. Bevington, P. R. (1969) *Data Reduction and Error Analysis for the Physical Sciences*, McGraw-Hill, New York.
29. Barshop, B. A., Wrenn, R. F., and Frieden, C. (1983) *Anal. Biochem. 130*, 134−45.
30. Espenson, J. H. (1981) *Chemical Kinetics and Reaction Mechanisms*, pp 65−66, McGraw-Hill, New York.
31. Russell, R., Karzai, A. W., Mehl, A. F., and McMacken, R. (1999) *Biochemistry 38*, 4165−76.
32. Farr, C. D., Galiano, F. J., and Witt, S. N. (1995) *Biochemistry 34*, 15574−82.
33. Farr, C. D., and Witt, S. N. (1999) *Cell Stress Chaperones 4*, 77−85.

BI0263208